AJAE

Open Access

Vol. 16, No. 2, 2021137, June 2022
doi: https://doi.org/10.5572/ajae.2021.137
ISSN (Online) 2287-1160, ISSN (Print) 1976-6912

Research Article

Characterization of Elemental Composition and Valence State of Cyclone-collected Aerosol Particles Using EDXRF and XAFS at Three Sites in Japan

Weidong Jing[1)], Katsutomo Saito[1)], Takuma Okamoto[1)], Hibiki Saito[1)], Kazuki Sugimoto[1)], Chiharu Nishita-Hara[2)], Keiichiro Hara[2),3)], Masahiko Hayashi[2),3)], Shuichi Hasegawa[4)], Tomoaki Okuda[1),*]

[1)]Faculty of Science and Technology, Keio University, 3-14-1 Hiyoshi, Kohoku-ku, Yokohama, Kanagawa 223-8522, Japan
[2)]Fukuoka Institute for Atmospheric Environment and Health, 8-19-1 Nanakuma, Jonan-ku, Fukuoka, Fukuoka 814-0180, Japan
[3)]Fukuoka University, 8-19-1 Nanakuma, Jonan-ku, Fukuoka 814-0180, Japan
[4)]Center for Environmental Science in Saitama, 914 Kamitanadare, Kazo, Saitama 347-0115, Japan

***Corresponding author.**
Tel: +81-45-566-1578
E-mail: okuda@applc.keio.ac.jp

Received: 18 November 2021
Revised: 8 February 2022
Accepted: 29 March 2022

ABSTRACT The valence state and concentration of metallic pollutants are important factors contributing to the health effects of respirable particulate matter (PM); however, they have not been well studied. In this study, coarse and fine powder samples of atmospheric PM were collected using a cyclone system at Kanagawa (KO), Saitama (SA), and Fukuoka (FU) in Japan in 2017. Energy dispersive X-ray fluorescence spectroscopy (EDXRF) was used to measure the concentrations of nine metallic elements (Ti, V, Cr, Mn, Fe, Ni, Cu, Zn, and Pb), and X-ray absorption fine structure (XAFS) spectroscopy was used to analyze the valence states of target elements (Cr, Mn, Fe, Cu, and Zn). The EDXRF results indicated that the average contents of Fe, Ti, and Zn were much higher than those of the other six elements in all samples. The XAFS results showed that the major valence states of the elements were Cr(III), Mn(II), Fe(III), Cu(II), and Zn(II). The percentages of Mn(IV), Fe(II), and Cu(0) were higher in KO and SA samples than in FU samples. Mn(0) and Zn(0) were detected in some samples only, and Cu(I) was not detected in any samples. Correlation analysis, principal component analysis, and cluster analysis were performed on the EDXRF and XAFS data of the target elements. The source identification results showed that the sources of metal contaminants in the samples varied considerably between sampling sites and depended on the industrial structure and geographical location of the sampling area. Our findings on the different valence states of the elements may be important for determining the toxicity of PM at different locations.

KEY WORDS Cyclone, Powder form of aerosol particles, EDXRF, XAFS, Valence states, Source identification, Chemical speciation

1. INTRODUCTION

Particulate matter (PM) pollution is a serious issue worldwide. $PM_{2.5}$ (particle diameter < 2.5 μm) contributed to more than 4.3 million premature deaths worldwide in 2015 (Cohen *et al.*, 2017). Exposure to high PM concentrations can cause adverse health effects including decreased lung function and cardiovascular and respiratory diseases (Charlson *et al.*, 2016; Zanobetti *et al.*, 2014; Sun *et al.*, 2010).

Metals are important components in PM that can produce reactive oxygen spe-

cies (ROS) including hydroxyl radicals in vivo, which are more toxic and cause pro-oxidant and proinflammatory effects on the respiratory system (Gao *et al.*, 2020; Taghvaee *et al.*, 2019; Chirizzi *et al.*, 2017). The biological toxicity and carcinogenicity of heavy metals can vary for different valence states. For example, Cr(III) poses little or no threat to human health, while Cr(VI) is toxic and potentially carcinogenic (Sun *et al.*, 2015; Sheehan *et al.*, 1991). Vanadium(V) species (e.g., V_2O_5) are particularly toxic and have mutagenic effects. Cohen *et al.* (2007) compared several forms of vanadium and demonstrated that the vanadate [V(V)] species had the greatest biological effects. Therefore, the valence states of metals should also be measured in addition to the metal concentrations in PM samples. In this study, we used energy-dispersive X-ray fluorescence (EDXRF) to analyze element concentrations in atmospheric PM, which allows rapid and non-destructive detection for elements concentration in a sample, and X-ray absorption fine structure (XAFS) spectroscopy, X-ray absorption near-edge structure (XANES) spectra mainly, to analyze the valence states of target metals in the PM samples (Saito *et al.*, 2020; Zhang, 2003; Huggins and Huffman, 2002).

Previous studies typically collected PM samples using filters made from different materials (such as quartz fiber or PTFE) with a low/high volume air sampler (Shahpoury *et al.*, 2021; Sugiyama *et al.*, 2020; Shimada *et al.*, 2019). However, in vivo or in vitro studies that used filters to collect PM may not reflect realistic biological reactions of health effects. First of all, high volume sampler, which is widely used for filter-samples collection, doesn't offer the separation collection of gas and particle-phase in general, gaseous compounds may be adsorbed to quartz fiber filters, thus resulting in a positive bias in the measured particle-phase concentration (Parshintsev *et al.*, 2011; Hering *et al.*, 1990). The study pointed that volatile organics may adsorb onto filter materials in the high volume sampler and undergo subsequent on-filter oxidation and sulfation resulting in the formation of both organic acids and organosulfates (Kristensen *et al.*, 2016). Additionally, the extraction of $PM_{2.5}$ collected by filters can alter particle properties. There are potential extraction artifacts such as compositional biases in the extracted PM, volatilization losses, and contamination with filter material (Roper *et al.*, 2019; Van *et al.*, 2015). Besides, particles collected and entangled in the filters are difficult to be removed without contaminating by the filter materials, and thus not suited for the following exposure experiments. Therefore, powder samples collected using a cyclone without filters are superior to aerosol samples adsorbed on a filter for studying cellular exposure and PM toxicity.

Cyclonic separation with an impactor enables the collection of $PM_{2.5}$ in "powder form" (Okuda *et al.*, 2018, 2015; Okuda and Isobe, 2017). PM is classified by an impactor, enters the cyclone device, and is collected at an inner wall of the cyclone and an attached bottle. Honda *et al.* (2020) studied the performance of two kinds of particles collected by cyclonic separation and filtration methods in cell exposure experiments. $PM_{2.5}$ collected using cyclonic separation has more significant effects for secreting of interleukins 6 and 8 (IL-6, IL-8) from airway epithelial cells, and expressing of the cluster of differentiation 86 (CD86) and dendritic and epithelial cells 205 (DEC 205) on antigen-presenting cells, comparing with the effects of filter-collected $PM_{2.5}$. Besides, powder samples collected by cyclone increased inflammatory cytokine levels and induced lung inflammation in vivo. The results suggested that crude $PM_{2.5}$ collected using cyclonic separation caused stronger biological responses than filter-collected $PM_{2.5}$. It was possibly due to the co-existence of particles in the exposure experiment had a significant effect rather than the exposure of extracts of particles without particles themselves. Another study compared the cytotoxicity and inflammatory potential of $PM_{2.5}$ collected by a cyclone from three Asian cities, by measuring cytokines such as interleukin (IL)-6 and IL-8 (Chowdhury *et al.*, 2019). Ogino *et al.* (2018, 2016) administered a mixture of powder particles and saline intranasally to NC/Nga mice for five consecutive days, collected bronchoalveolar lavage fluid (BALF) from the mice, and analyzed them for airway hyperresponsiveness (AHR). The studies showed that $PM_{2.5}$ increased AHR and cell numbers of eosinophils in BALF, and that $PM_{2.5}$ collected by the cyclone system could induce asthma-like airway inflammation. A recent study analyzed lung sections of mice that underwent tracheal injection of particles in a crude PM dispersion liquid (Sagawa *et al.*, 2021). The results showed that PM exposure increased the expression of angiotensin-converting enzyme 2 (ACE2) and transmembrane protease serine-type 2 (TMPRSS2) in alveolar cells and macrophages, which are required for the entry of severe acute respiratory syndrome coronavirus 2 (SARS-CoV-2) into host cells, thereby demonstrating that PM exposure may adversely affect the manifestation and progression of COVID-19. These studies have

shown that powder particles collected by the cyclone have better operability than filtration in cell exposure experiments and in vivo experiments.

Another advantage of cyclone-collected aerosol particles is that the pelletized powder form of particles is suitable for XAFS analysis. In contrast, aerosol particles layer on the filter which collected by filtration method would be too thin that it is difficult to obtain a sufficient quality of XAFS signals relative to the background noise (Saito *et al.*, 2020).

The objectives of this research were to (i) measure the content of metal elements in powder aerosol samples of different sizes collected by a cyclone using EDXRF; (ii) understand the characteristics of the valence states of target metals by XAFS, and (iii) identify the sources of target metals at three sampling sites in Japan based on the source identification models. These results can provide more detailed information for understanding the correlation between the contamination properties of heavy metals in atmospheric PM samples and their oxidation potential in further cell exposure experiments.

2. EXPERIMENTAL

2.1 Sample Collection

We collected aerosol samples at three sites in Japan: Fukuoka University (FU), Keio University (KO), and the Center of Environmental Science in Saitama (SA). Fig. 1 shows the locations of the sites. Fukuoka University (33.550°N, 130.364°E) is in Fukuoka Prefecture in southwestern Japan, which is close to the East Asian continent.

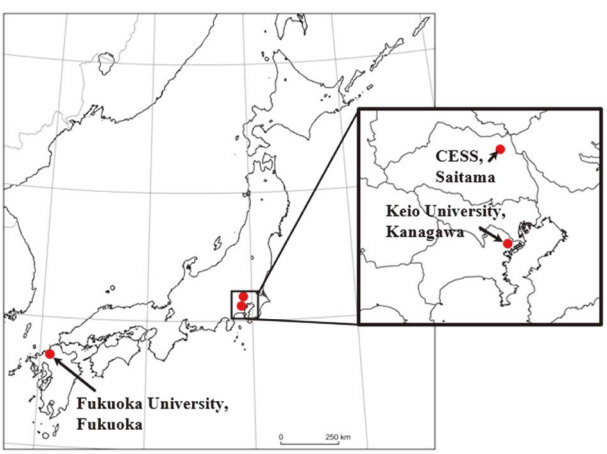

Fig. 1. Location map of sampling sites.

This unique location is suitable for observing the effects of long-range transport on air pollution. Keio University (35.555°N, 139.656°E) is located in Kanagawa Prefecture on the east coast of mainland Japan. Kanagawa Prefecture is part of the Tokyo metropolitan area, has the largest port in the country, and is one of the four major industrial zones in Japan. The Center of Environmental Science in Saitama (CESS) (36.086°N, 139.560°E) is in an inland area with high agricultural and industrial production. These three sampling sites have different sources of air pollutants due to different geographical locations and industrial activities.

We used a high-flow simultaneous sampling system that combined the virtual impactor and cyclone to collect atmospheric PM at a flow rate of 1,200 L/min. Particles with diameters smaller than 2.5 μm were classified as fine particles (PF) and particles with diameters larger than 2.5 μm were classified as coarse particles (PC). Details of the particle collection instrument are provided in our previous studies (Okuda *et al.*, 2018, 2015). Table 1 shows the mass of PM during the sampling period and the meteorological conditions (JMA, 2021) at the sampling sites.

2.2 EDXRF Analysis

We measured element concentrations in the atmospheric PM by using an EDXRF analyzer (EDXL 300, Rigaku Corp., Japan) (Okuda *et al.*, 2018, 2013) with a solid-state detector (SSD). The 20 mg of powder samples was placed onto the 300 mg of cellulose powder, and then the layered powder was pressed into pellets of Φ13 mm × 0.5 mmt by 50 kN pressure for testing. Standard material of urban aerosol particles (CRM#28) with known metal contents was also pelleted and analyzed for calibration. The pelletized samples were analyzed by EDXRF in approximately 1 Pa of vacuum, and the analysis time was 15 min per a sample. The quantification was achieved with a fundamental parameter coupled with O-Balance method. The ratio of measured and certified values for each element ($n = 5$) was generally in the range of 0.8–1.2, and measurement precision, represented as the coefficient of variation (= standard deviation/mean), was less than 20% (Okuda *et al.*, 2018).

2.3 XAFS Spectra Analysis

We mainly used XANES to probe the valence states of the absorbing atoms, which were measured at the Kyushu

Table 1. Amount of collected particles and meteorological data during the sampling period for three sampling sites.

	Date	Season	Volume (m^3)	Fine particles (mg)	Coarse particles (mg)	Total rainfall[a] (mm)	Average relative humidity (%)	Average sunshine duration (h)
Kanagawa (KO)	2/15–3/10	Winter	42648.0	434.0	619.2	26.5 (2/16–3/10)	56.4	5.8
	5/10–6/06	Spring	51614.2	238.0	267.3	97.5 (5/11–6/5)	70.8	10.9
	7/14–8/07	Summer	47068.5	115.4	105.3	176 (7/16–8/10)	65.6	4.1
	10/18–11/16	Autumn	56424.1	172.5	75.4	446 (10/16–11/15)	74.5	4.7
Saitama (SA)	2/17–3/15	Winter	49054.6	290.4	212.9	13.5 (2/16–3/15)	46.0	6.3
	5/10–6/06	Spring	50639.0	200.4	133.5	50.5 (5/11–6/5)	62.6	7.3
	7/14–8/07	Summer	44848.6	95.8	54.1	69.0 (7/16–8/10)	74.8	3.6
	10/20–11/15	Autumn	48454.2	148.7	118.5	323 (10/21–11/15)	67.6	5.7
Fukuoka (FU)	2/16–3/21	Winter	61613.2	182.5	92.0	42.0 (2/16–3/20)	59.9	5.6
	5/11–6/08	Spring	52442.5	167.7	136.8	65.5 (5/11–6/10)	63.8	9.1
	7/21–8/17	Summer	50631.3	97.5	55.5	53.5 (7/21–8/15)	75.6	8.3
	10/19–11/16	Autumn	52280.6	195.8	55.4	65.5 (10/21–11/15)	69.6	6.1

All meteorological data were obtained from JMA, 2021. For KO, rainfall data were from the Hiyoshi monitoring station, while relative humidity and sunshine duration data were from Yokohama station. For SA, rainfall and sunshine duration data were from Kuki station, and relative humidity was from Kumagaya station. For FU, meteorological data were from Fukuoka station.
[a]The date in parentheses indicates the statistical date of the station.

Synchrotron Light Research Center (SAGA-LS) using Beam Line 11 and 15 (BL-11 and BL-15). This ensured the quality of the continuous spectrum by performing the XAFS measurement on synchrotron radiation (Saito *et al.*, 2020). The valence states of target metals in the PC sample collected in the winter at FU could not be determined, as a large proportion of this sample was used for other experiments and the remaining amount was not enough to do the XAFS measurement.

XANES is a fine structure in the absorption spectrum that appears in the narrower energy range (−10 eV to + 40 eV) near the absorption edge. Absorbance increases sharply at a certain energy value in the XAFS spectrum, which is referred to as the absorption edge. In this study, the midpoint of the rising edge of the absorption peak was uniformly defined as the absorption edge of the samples, while the pre-edge and post-edge lines were drawn with the energy range of −150 eV to + 30 eV with the absorption edge as the center point. The absorbance on the pre-edge line was 0 ($E_0 = 0$), and the absorbance on the post-edge line was 1 ($E_1 = 1$). The absorption peak was located above the post-edge line, so its absorbance was greater than 1.

Energy calibration of XAFS measurement has been achieved using a common method as follows. A foil of the target element was placed downstream of the sample, in

the path of the X-rays and between the 1st and 2nd transmitted intensity monitors, and then the absorption spectrum was obtained by taking the natural logarithm between the 1st signal to the 2nd. The energy position of the known features in the spectrum was used as calibration for the experiment so that the energy scale of the samples was adjusted.

Metallic standard compounds (Mn, MnO, MnO_2, Fe, FeO, Fe_3O_4, $Fe_2O_3(\alpha, \gamma)$, FeOOH, Cu, Cu_2O, CuO, $CuCl_2$, $CuSO_4$, CuS, Zn, ZnO, $Zn(OH)_2$, $ZnFe_2O_4$, $ZnSO_4$, and $Zn(NO_3)_2$) were used to carry out the chemical speciation for each metallic compound by using the linear combination fitting (LCF) method. Each standard compound was mixed well with boron nitride (BN) for 20 min in a mortar, then it was pressed into a pellet similar to the aerosol samples. For XAFS spectra analysis, we measured the XAFS spectra of the standards substances with the different valence of the target metal at first, and then performed a linear fit using the least-squares method after obtaining the XAFS spectra of the target elements in the sample to calculate the valence ratio of the target metal in the sample. Normalization of the experimental data and the linear fitting calculation using the least-squares method for valence ratio were done using Athena software (ver. 0.9.26), and the detailed procedures are described in a previous paper (Saito *et al.*, 2020). The R-factors, which were generally used for the evaluation of fitting results, ranged 0.01–0.06 for Mn (except for SA-winter-PC, 0.28), smaller than 0.002 for Fe, 0.002–0.007 for Cu, and 0.002–0.02 for Zn. For Zn speciation, since the spectra for ZnO and $Zn(OH)_2$, and also $ZnSO_4$ and $Zn(NO_3)_2$, were very similar, we used only Zn, ZnO, $ZnFe_2O_4$, and $ZnSO_4$ for the LCF analysis.

2.4 Indices of Source Identification

Enrichment factors (EFs) were used to evaluate the air quality in terms of heavy metals and indicate the contribution of anthropogenic emissions to the atmosphere. Here, EFs are defined as

$$EF = \frac{C_i^{PM}/C_X^{PM}}{C_i^{crust}/C_X^{crust}} \quad (1)$$

where C_i^{PM} is the concentration of element i in the PM samples, and C_X^{PM} is the concentration of X as a reference element in the PM samples. C_X^{crust} indicates the assumption that the dominant source of X in PM originated from the natural crust. C_i^{crust} is the average elemental concentration in the crust. In this equation, we used the average chemical profile of continental crust data from Taylor (1964) and chose Ti as the reference element instead of Al (Loska *et al.*, 1997), because we focused on transition metals and heavy metals that were potentially more harmful and did not show the aluminum contents in this study. An EF of <10 suggests that crustal sources are mainly natural, and an EF of >10 suggests strong enrichment from non-crustal sources (Ny and Lee, 2010; Al-Momani *et al.*, 2005).

Principal component analysis (PCA) was used to identify likely sources of the metallic elements. We normalized all data using the z-score method before analysis, and we rejected factors that contributed less than 5% to the variance.

Cluster analysis (CA) was used to indicate the potential emitting sources of the different metals in the samples detected by EDXRF and XAFS. We combined CA and PCA results for greater confidence in the source identification. The grouping of CA results was chosen on the basis of a dendrogram using the average linkage method with Euclidean distances. We used Origin software (version: OriginPro 2018C) to perform these analyses.

3. RESULTS AND DISCUSSION

3.1 Metallic Element Concentration in Aerosol Particles

Table 2 presents the concentrations of nine metallic elements in aerosol particles detected by EDXRF. Note that all data were expressed in the mass concentration (μg/g) in the original aerosol particles. The concentration of Ti ranged between 1,060 and 3,780 μg/g in KO, between 652 and 4,170 μg/g in SA, and between 246 and 1,680 μg/g in FU. In terms of seasonal variations, the concentration of Ti in all samples, except for PF collected in KO, tended to be higher in winter and spring and lower in summer and autumn. The concentrations of V and Ni were more constant, with overall average concentrations of 62 and 63 μg/g, respectively. The overall average concentration of Pb in KO samples (159 μg/g) were much higher than in SA and FU samples (59.3 and 69.6 μg/g). The characteristic concentration distributions of V, Ni, and Pb in the different sized particles were similar, higher in PF compared with PC in samples from SA and FU, while we observed the opposite in the KO samples.

Cr, Cu, and Mn are highly related elements with oxida-

Table 2. Concentrations of heavy elements in aerosol particles detected by EDXRF. (unit: μg/g)

			Ti	V	Cr	Mn	Fe	Ni	Cu	Zn	Pb
KO	Fine particles	Winter	2,810	72.7	104	677	29,100	62.9	264	859	58.4
		Spring	1,140	67.9	52.5	405	13,800	43.2	152	567	51.4
		Summer	1,220	89.7	114	413	14,600	57.2	201	565	53.6
		Autumn	1,490	74.9	102	519	17,500	53.7	274	804	74.1
		Average	1,660	76.3	93.1	503	18,800	54.3	223	699	59.4
		EF	1.0	1.5	2.5	1.4	1.0	1.9	**10.7**	**26.4**	**12.1**
	Coarse particles	Winter	3,230	102	154	866	38,200	49.8	642	1,710	140
		Spring	3,780	128	185	1,330	53,700	134	1,280	7,350	593
		Summer	1,060	48.2	76.5	399	14,000	32.6	403	3,200	175
		Autumn	1,750	85.1	126	555	20,000	44.9	531	1,510	126
		Average	2,460	90.8	135	787	31,500	65.3	714	3,440	258
		EF	1.0	1.2	2.4	1.5	1.1	1.6	**23.3**	**88.2**	**35.6**
SA	Fine particles	Winter	2,520	69.9	125	616	25,300	64.2	162	896	81.3
		Spring	4,170	150	153	1,170	44,800	92.6	450	2,060	178
		Summer	791	47.7	1,030	289	10,600	388	92.2	303	28.4
		Autumn	1,340	27.2	323	473	10,200	111	109	578	42.6
		Average	2,210	73.6	200	637	22,700	164	203	960	82.5
		EF	1.0	1.1	8.1[a]	1.3	1.0	4.4	7.4	**27.4**	**12.7**
	Coarse particles	Winter	1,520	40.6	71.8	385	14,000	21.0	160	447	27.9
		Spring	1,900	51.9	59.7	493	20,400	41.2	155	865	75.1
		Summer	652	25.5	40.1	146	5,430	11.2	94.2	258	15.8
		Autumn	1,020	23.0	48.6	344	7,880	17.6	118	418	25.2
		Average	1,280	35.2	55.1	342	11,900	22.7	132	497	36.0
		EF	1.0	0.9	1.9	1.2	0.8	1.1	8.3	**24.5**	9.6
FU	Fine particles	Winter	1,360	85.3	86.9	438	13,800	74.7	211	1,142	241
		Spring	1,680	59.9	105	393	15,900	74.1	105	559	94.8
		Summer	246	35.7	32.7	77.3	2,200	17.6	34.0	225	36.8
		Autumn	484	20.4	31.2	87.7	4,600	9.6	54.0	144	18.9
		Average	942	50.3	63.9	249	9,120	44.0	101	518	98.0
		EF	1.0	1.7	3.0	1.2	0.9	2.7	8.6	**34.5**	**35.2**
	Coarse particles	Winter	–	–	–	–	–	–	–	–	–
		Spring	1,310	47.9	37.9	280	12,500	28.8	85.7	327	55.3
		Summer	276	25.5	26.7	59.4	2,310	6.9	25.5	152	17.9
		Autumn	420	35.7	32.4	103	3,870	17.6	40.2	225	50.5
		Average	668	36.4	32.4	147	6,250	17.8	50.5	235	41.2
		EF	1.0	1.8	2.1	1.0	0.8	1.6	6.1	**22.1**	**20.9**

All data were expressed in the mass concentration (μg/g, with three significant figures) in the original aerosol particles.
– Not analyzed.
[a]Irregular data were eliminated during the calculation of EF for Cr in SA PF samples.

tive potential, which is a measure for the toxicity of atmospheric PM (Szigeti *et al.*, 2015; Janssen *et al.*, 2014; See *et al.*, 2007). Fe and Zn also have a relatively high association with oxidation capacity (Gao *et al.*, 2020; Wang *et al.*, 2018; Stoiber *et al.*, 2013), and they were present at relatively high atmospheric concentrations (Table 2). Therefore, we selected these five elements as the target elements to further investigate their pollution properties and chemical characteristics.

3.1.1 Cr

The concentration of Cr in PC and PF collected in KO and FU was constant, with averages of 114 ± 42 μg/g and 50 ± 32 μg/g in all samples from the two locations,

respectively. In contrast, the concentration of Cr in PF collected in SA in summer reached 1,030 μg/g, which was much higher than in the other samples. The high Cr concentration may have resulted from local emissions during the sampling period. Comparison of the results of other samples showed that the concentration of Cr was not higher in PF than in PC. Therefore, this high concentration of Cr was irregular, and the data from this sampling time was removed in subsequent analyses.

3.1.2 Mn

The concentrations of Mn in the samples from KO ranged between 399 and 1,330 μg/g and were close to the soil background value (950 μg/g). Mn concentrations in SA and KO samples were similar, but the particle size distributions were different. In KO samples, Mn concentration was higher in PC than in PF, while the opposite was observed in SA samples. Additionally, Mn concentrations for the two particle sizes from both SA and KO were high in winter and spring. Mn concentration was even lower in samples from FU than in those from KO and SA during the same sampling period, especially in samples collected in summer (77.3 μg/g in PF and 59.4 μg/g in PC). Note that not only Mn but the other crustal elements such as Ti was also low in the concentration in aerosol samples collected in summer in FU. One possible speculation for this result is that the Asian dust transportation in summer in Fukuoka may weak in compared to the other seasons (Kaneyasu *et al.*, 2014).

3.1.3 Fe

The average concentration of Fe was the highest among the nine metallic elements across the three sites. Fe concentration was the highest in samples from KO (25,100 μg/g), followed by SA (17,300 μg/g) and FU (7,680 μg/g). For samples from the same location, Fe concentration showed trends similar to those of Mn for both particle sizes and particle size concentration distributions.

3.1.4 Cu

Cu concentrations in all samples were relatively low except in PC of KO samples (714 μg/g on average). Cu concentrations were comparable in PC and PF in SA (203 vs. 132 μg/g) and FU samples (101 vs. 50.5 μg/g), while there were large differences for KO samples. Cu concentrations in the rest of the samples were higher in winter and spring, except for PF in KO samples.

3.1.5 Zn

Zn concentrations in PC and PF from KO samples were considerably different. Trend in Zn concentration were similar to that in Mn, Fe, and Cu. Zn concentration in PC from KO was high (3,440 μg/g) compared with other samples from SA and FU (497 and 235 μg/g, respectively).

3.2 Valence State of Target Elements

The XAFS spectra of each element for the standard materials, representative aerosol samples, and corresponding LCF results with the lowest R-factors among the samples are shown in Fig. 2. The percentages of different valence states of target metals detected by XAFS are shown in Fig. 3. We only examined the valence states of Mn, Fe, Cu, and Zn, as those of Cr were explored in our previous study (Saito *et al.*, 2020).

3.2.1 Mn

Mn(II) was the major component in all aerosol samples at averages of 60.9%, 73.8%, and 85.1% for KO, SA, and FU, respectively. Mn(0) was detected in some PC samples from KO and SA at under 10%. Mn(IV) accounted for a relatively large proportion of aerosol samples collected in KO and SA (37.6% and 25.8% on average), especially in samples collected in winter. These results were generally consistent with a previous study that reported the oxidation state of Mn in the aerosol or road dust samples were approximately 2.2–2.6 (Bardelli *et al.*, 2011; Ohta *et al.*, 2006).

3.2.2 Fe

The major valence state of Fe in the aerosol samples was Fe(III). The average proportions of Fe(III) in KO, SA, and FU samples were 70.4% (n = 8), 79.8% (n = 8), and 86.7% (n = 7), respectively. There was more Fe(II) in KO samples (23.5% average) than in SA samples (12.9% on average) and FU samples (8.4% on average). Fe(III) concentration was the highest but Fe(II) concentration was the lowest in FU samples. This may be because Fe(II), which was more reactive valence state than Fe(III), was oxidized during the long-range transport from the Asian continent. This is also supported by Takahashi *et al.* (2011) which showed that that the ratio of Fe(III) to total Fe increases during atmospheric transport from the Taklimakan desert to Japan. In contrast, there was more Fe(II) in SA and KO samples due to greater local emissions of aerosol particles containing

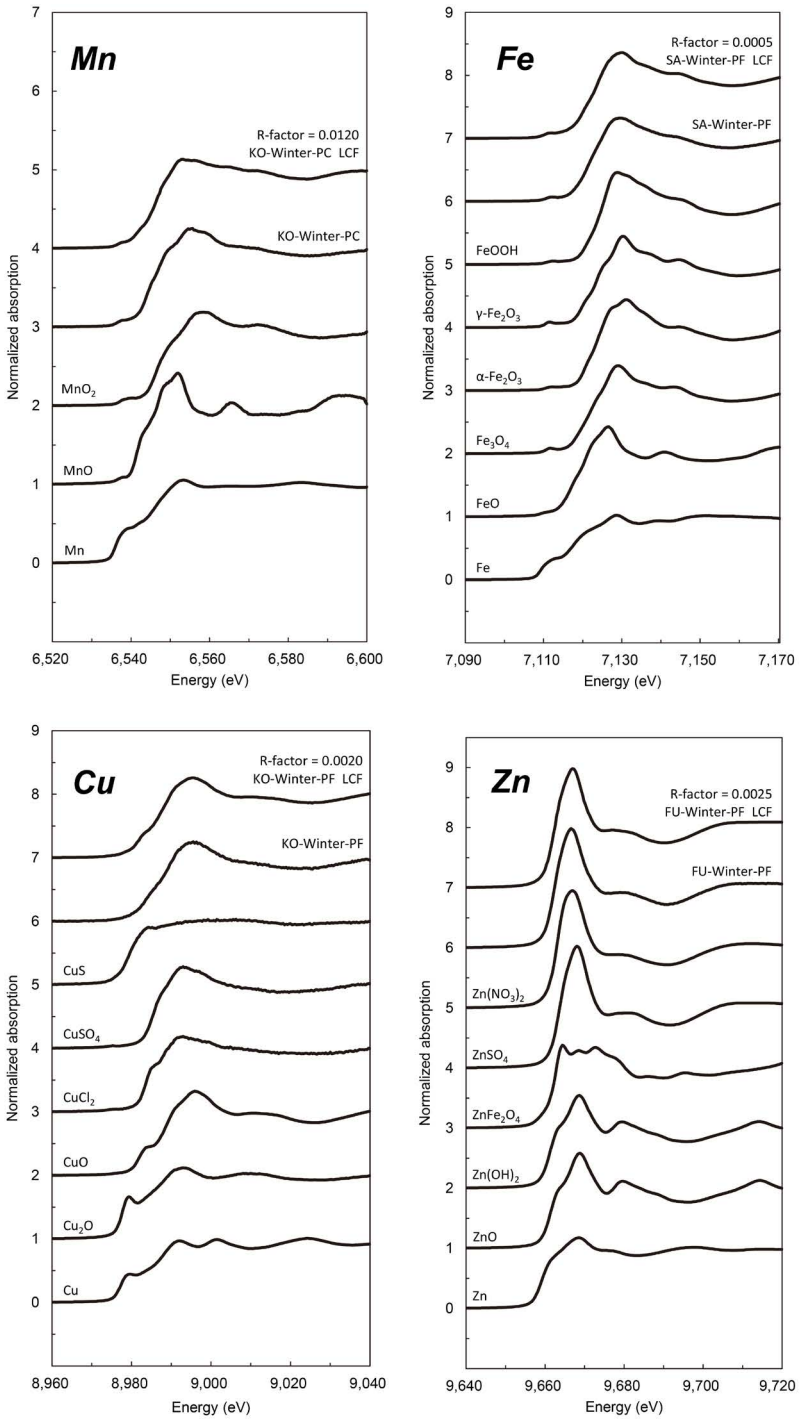

Fig. 2. The XAFS spectra of each element for the standard materials, representative aerosol samples, and corresponding linear combination fitting (LCF) results.

Fe(II). Moreover, Fe(0) was not detected in five samples including PF from KO in autumn and PC from SA in spring. Fe(II) was not detected in PC from SA in summer and PF from FU in autumn.

3.2.3 Cu

Cu(II) was the main component of the particles at all locations and sizes. The average percentage of Cu(II) was 92.1% in KO, 88.0% in SA, and 99.4% in FU. The pro-

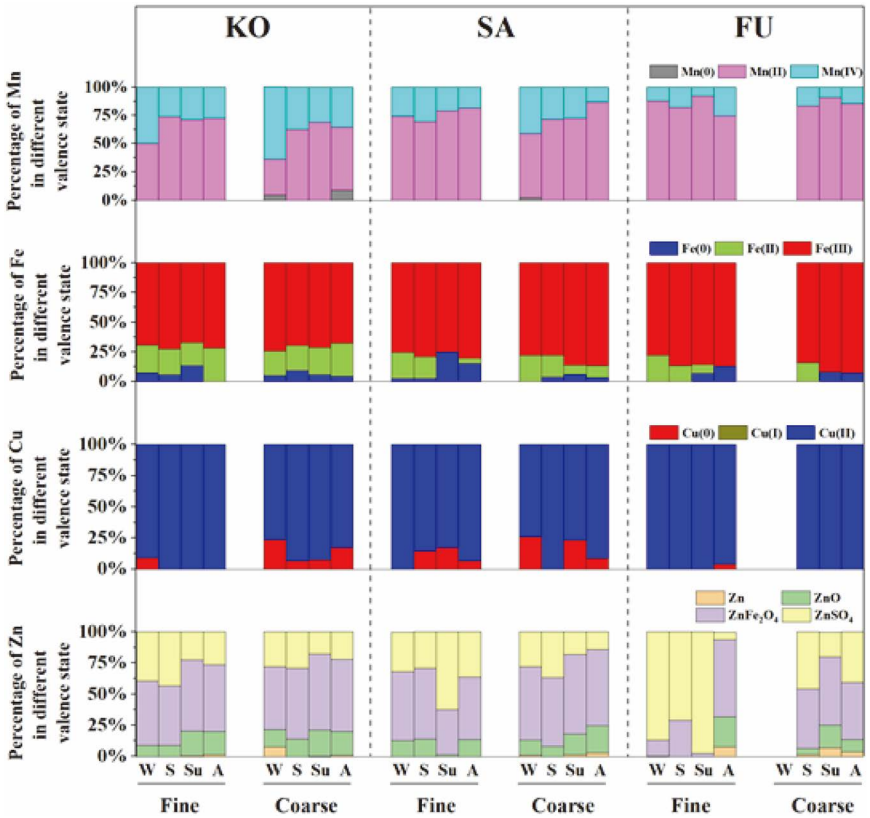

Fig. 3. Percentage composition of different valence states of target metals (Mn, Fe, Cu, and Zn) in fine and coarse particles at three sites in Japan.

portion of Cu(0) was larger in PC at KO (13.6% average) and SA (14.4% average), and it was only detected in PF from all FU samples collected in autumn. Cu(I) was not detected in any sample.

3.2.4 Zn

Zn(II) was the major chemical valance of Zn in all samples (98.8% in KO, 99.4% in SA, and 97.2% in FU). In order to make more detailed discussion, the chemical speciation results for Zn are presented in Fig. 3. The major Zn components were $ZnFe_2O_4$ and $ZnSO_4$. The proportion of $ZnFe_2O_4$ was higher than $ZnSO_4$ in all samples (54% vs 31.3% on average) except the fine particles collected in FU site (26.7% vs 65.3% on average). In addition, ZnO existed in all samples except the fine samples collected in spring and summer at FU but at a low amount (12.3% on average). Zn(0) was detected only in some particles and the average proportion in FU samples were three times than others (2.8% to 0.9%). Overall, the Zn chemical speciation result for FU was unique. Note that when we changed $ZnSO_4$ to $Zn(NO_3)_2$ as the standard spectrum for the LCF analysis, the result was very similar to the original result.

3.3 Source Identification

EFs, correlation analysis, PCA, and CA were applied to identify the potential sources of metallic elements in aerosol samples from three sampling sites.

3.3.1 Enrichment Factors (EFs)

EFs for metals in the particle samples were calculated by using the average concentrations to investigate the potential sources of metallic elements that were emitted from natural or anthropogenic sources. The results are summarized in Table 2.

The results showed that Ti, V, Cr, Mn, Fe, and Ni had EF values in the range of 0.8–4.4, which suggests that these metals were derived from crustal contribution and part of anthropogenic influences. The EFs of Zn were higher than 10 in all samples at three sites. The values of Pb were also higher than 10 in all samples except for PC collected in the SA site. The EF values of Cu in the KO

samples are also higher than 10 and those in the other two sampling sites are also much higher than the reference values as crustal sources. This suggests that the contribution of soil to these elements was much smaller than those of anthropogenic sources. Pb has been used in marker compounds for coal combustion and non-ferrous metal smelters (Ny *et al.*, 2010; Okuda *et al.*, 2008). Additionally, the presence of Pb in atmospheric air is related to vehicular and industrial emissions (i.e., burning of fossil fuels) (Alves *et al.*, 2020; Hassanvand *et al.*, 2015). Xu *et al.* (2012) listed vehicular emissions as one of the main sources of Pb in the environment of Xi'an, China, even after the use of Pb-containing gasoline was prohibited. Zn is used to make automotive brakes and tire rubber (which contains 1% Zn as it acts an activation agent for the sulfurization of rubber), and Zn is also added to automobile engine oil (Grigoratos *et al.*, 2015; Iijima *et al.*, 2007).

3.3.2 Correlation Analysis

Fig. 3 shows the XAFS results on the valence states of the five trace metals in aerosol particles. The concentration of each valence state was calculated from its percentage and the total metal concentration from Table 2. These values were used in a correlation analysis to investigate the potential emission sources of aerosol particles at the three sites (Table 3). *Z*-score normalization was applied to all data to standardize different magnitudes into a uniform measure before correlation analysis. In addition, *t*-tests were performed to determine the statistical significance of the correlation analysis results (Table 3) in order to reduce calculation errors from the small number of samples ($n = 4$). Correlations between an element and its valence states are not discussed as they are not independent, since valence state concentrations were calculated using the element concentrations and valence state percentages.

The concentration of Cr in PF in summer SA samples may be anomalous, as previously discussed. Therefore, we excluded the data for this sampling period to keep the data constant when performing the correlation analysis between Cr and other elements. These correlation coefficients are indicated in Table 3b by a gray background. However, these correlation coefficients are less accurate (e.g., $r^2 = 1.00$ between Cr(III) and Mn) because of the reduced sample size and will not be used for source analysis. Similarly, the correlation analysis of elements in FU PC samples was excluded because of the lack of EDXRF and XAFS data on FU PC samples collected in winter.

As shown in Table 3, there were significant correlations between Mn(IV) and Ti, and the correlation of Fe(II) and Fe(III) with Ti and Mn for all samples. Ti, Mn, and Fe are all typical crustal enrichment elements, and the EFs for both Mn and Fe were close to 1 (Table 2), which indicates that Mn and Fe mainly originated from the soil. There is research pointed that small-sized particles were emitted from vehicle exhausts as a result of engine combustion (Tanner *et al.*, 2008), and Lu *et al.* (2009) stated that the principal source of Mn and Pb in street dust is automotive emissions. Therefore, the high correlations of Mn with Cu, Zn, and Pb in SA fine particles indicated that automotive emissions might be one anthropogenic source of Mn.

Zn is the largest metallic portion emitted from electric arc furnace dust, which can reach 7%–40% of total metal emissions. Vapor zinc is emitted out from the furnace as compounds like ZnO and $ZnFe_2O_4$ with other gaseous or particulate compounds generated during steelmaking reactions (Oustadakis *et al.*, 2010; Xia and Picklesi, 2000), while Mn is derived from franklinite ($(Zn, Mn^{2+}, Fe^{2+})(Fe^{3+}, Mn^{3+})_2O_4$), and Cr is richer in the dust from stainless steelmaking than in that from carbon steelmaking (Omran and Fabritius, 2017; Havlík *et al.*, 2006; Sofilić *et al.*, 2004). Manno *et al.* (2006) stated that heavy metals such as Zn and Ni are highly abundant in urban areas and industrial sites, and major sources of V have been identified as combustion of residual fuel such as ships and refinery plants (Agrawal *et al.*, 2008a, 2008b; Vallius *et al.*, 2003). Therefore, the strong correlations of Zn, Mn, Fe, and Cr with Ni ($r^2 = 0.801$–0.975, $p < 0.05$) and V ($r^2 = 0.814$–0.965, $p < 0.05$) in aerosol particles at KO and FU sites indicates that they were likely emitted from industrial production in the Keihin and Kitakyushu industrial areas, where also are important ports.

Cu and Zn are known as wear-generating elements, as Cu can be emitted from the wear of engine parts, fuel, and oil leakage (Hassan, 2012; Yuen *et al.*, 2012), while Zn can be derived from tire abrasion, brake wear, and corrosion of vehicle parts (López *et al.*, 2011). Previously deposited Pb in the soil may be re-suspended in road dust (Taylor and Kruger, 2020; Chen *et al.*, 2019; Jeong *et al.*, 2018; Amato *et al.*, 2014; Chen *et al.*, 2014). This explains the significant correlations between Cu(II), Zn(II), and Pb. Furthermore, a previous chemical characterization study of brake wear particles showed that Fe existed in both fine and coarse fractions, while TEM analysis revealed the presence of maghemite (γ-Fe_2O_3),

Table 3. Pearson correlation analysis of valence state concentrations for different particle size samples.

a. KO

Fine particles	Cr(0)	Cr(III)	Mn(II)	Mn(IV)	Fe(0)	Fe(II)	Fe(III)	Cu(II)	Zn(II)
Ti	**0.952***	0.091	0.401	**0.998****	0.461	0.945	**0.996****	0.483	0.816
V	−0.125	0.816	−0.298	−0.228	0.445	−0.348	−0.306	0.110	−0.320
Cr	0.328	**0.958***	0.312	0.351	0.397	0.356	0.328	0.699	0.406
Mn	0.858	0.158	0.598	**0.957***	0.272	**0.994****	**0.987***	0.647	0.926
Fe	0.943	0.112	0.428	**0.996****	0.442	**0.953***	**0.997****	0.511	0.833
Ni	0.742	0.702	0.309	0.751	0.610	0.681	0.717	0.647	0.623
Cu	0.425	0.608	0.870	0.600	−0.076	0.806	0.671	**0.981***	0.913
Zn	0.601	0.247	0.856	0.778	−0.075	**0.958***	0.855	0.841	**1.000****
Pb	−0.163	0.446	0.949	0.071	−0.641	0.436	0.198	0.884	0.675
Coarse particles									
Ti	0.843	0.860	0.690	**0.957***	0.861	**0.968***	**0.988***	0.780	0.532
V	0.861	0.924	0.747	0.853	0.854	**0.980***	0.936	0.817	0.533
Cr	0.876	0.910	0.725	0.873	0.844	**0.977***	0.941	0.800	0.511
Mn	0.684	**0.962***	0.874	0.837	**0.971***	**0.991****	**0.981***	0.931	0.751
Fe	0.734	0.923	0.811	0.897	0.943	**0.987***	**0.997****	0.882	0.686
Ni	0.439	**0.979***	**0.988***	0.594	**0.983***	0.909	0.855	**0.999****	0.906
Cu	0.522	**0.988***	**0.967***	0.673	**0.991****	0.947	0.903	**0.992****	0.869
Zn	0.045	0.802	0.948	0.338	0.890	0.679	0.655	0.923	**1.000****
Pb	0.223	0.902	**0.990***	0.455	**0.951***	0.798	0.757	**0.979***	**0.981***

b. SA

Fine particles	Cr(0)	Cr(III)	Mn(II)	Mn(IV)	Fe(0)	Fe(II)	Fe(III)	Cu(II)	Zn(II)
Ti	0.863[a]	0.974	**0.977***	**0.982***	−0.638	**0.973***	**0.987***	**0.970***	**0.981***
V	0.900	0.989	0.912	**0.973***	−0.348	0.901	**0.980***	**0.972***	**0.955***
Cr	−0.286	−0.558	−0.517	−0.607	0.826	−0.896	−0.716	−0.558	−0.561
Mn	0.957	1.000	**0.998****	**0.993****	−0.536	0.914	**0.975***	**0.991****	**0.998****
Fe	0.853	0.969	**0.952***	**0.987***	−0.534	**0.967***	**0.999****	**0.977***	**0.975***
Ni	0.227	−0.072	−0.653	−0.532	0.938	−0.649	−0.525	−0.502	−0.569
Cu	0.970	0.998	**0.967***	**0.991****	−0.365	0.867	**0.971***	**0.997****	**0.988***
Zn	0.954	1.000	**0.993****	**0.997****	−0.500	0.913	**0.982***	**0.997****	**1.000****
Pb	0.928	0.997	**0.983***	**1.000****	−0.503	0.933	**0.993****	**0.997****	**0.997****
Coarse particles									
Ti	0.689	0.858	0.758	0.888	0.437	**0.968****	**0.987***	**0.969***	0.911
V	0.666	0.676	0.538	0.887	0.510	**0.965***	**0.964***	0.857	0.881
Cr	**0.971***	0.942	0.402	0.942	−0.199	0.857	0.699	0.661	0.470
Mn	0.562	0.883	0.910	0.751	0.417	0.851	0.915	**0.983***	0.883
Fe	0.629	0.766	0.715	0.863	0.541	0.964	**0.999****	**0.953***	0.943
Ni	0.368	0.612	0.808	0.671	0.754	0.839	**0.963***	**0.953***	**0.999****
Cu	0.882	**0.962***	0.614	**0.961***	0.095	**0.953***	0.874	0.852	0.709
Zn	0.329	0.606	0.840	0.635	0.767	0.812	0.950	**0.957***	**1.000****
Pb	0.264	0.509	0.780	0.590	0.829	0.778	0.927	0.912	**0.993****

magnetite ($FeO\text{-}Fe_2O_3$), and amorphous carbon in the nanoparticle fraction, as well as maghemite, magnetite, and hematite ($\alpha\text{-}Fe_2O_3$) in the fine fraction (Grigoratos *et al.*, 2015). Hence, the Fe produced by brake wear emissions from cars is mainly in the form of compounds. However, the correlation of Fe(II) and Fe(III) with Zn

Table 3. Continued.

c. FU

Fine particles	Cr(0)	Cr(III)	Mn(II)	Mn(IV)	Fe(0)	Fe(II)	Fe(III)	Cu(II)	Zn(II)
Ti	0.666	**0.993****	0.927	**0.994****	−0.653	0.890	**0.999****	0.717	0.713
V	0.591	0.821	**0.953***	0.710	−0.834	**0.974***	0.755	0.933	**0.977***
Cr	0.767	**0.999****	0.938	**0.969***	−0.762	0.906	**0.985***	0.709	0.733
Mn	0.628	**0.964***	**0.998****	0.918	−0.748	**0.988***	0.940	0.884	0.894
Fe	0.644	**0.992****	0.946	**0.989***	−0.658	0.914	**0.996****	0.759	0.752
Ni	0.734	**0.976***	**0.986***	0.915	−0.823	**0.972***	0.942	0.825	0.857
Cu	0.272	0.726	0.904	0.667	−0.570	0.931	0.693	**1.000****	**0.982***
Zn	0.397	0.743	0.921	0.651	−0.696	**0.951***	0.689	**0.986***	**1.000****
Pb	0.336	0.686	0.886	0.590	−0.661	0.922	0.629	**0.985***	**0.996****

*$p < 0.05$, **$p < 0.01$
[a]Correlation coefficient between contaminants without irregular data in SA samples collected in summer.

Table 4. Varimax rotated factor loadings (only those with values ≥ 0.3 are listed) for XAFS data of target metals from three sites.

Components	KO			SA		FU			
	PC1	PC2	PC3	PC1	PC2	PC1	PC2	PC3	PC4
Cr(0)		0.53			0.65				0.30
Cr(III)			0.76		0.45	0.35			
Mn(II)	0.33			0.39		0.38			
Mn(IV)	0.32	0.48		0.38		0.35		0.50	
Fe(0)	0.34				0.50			0.52	0.71
Fe(II)	0.36			0.36		0.37			
Fe(III)	0.37			0.39		0.35		0.43	
Cu(II)	0.36			0.38		0.34	0.36		0.33
Zn(II)	0.32			0.39		0.34			0.37
Eigenvalues	6.9	1.11	0.47	6.33	2.23	6.99	0.84	0.57	0.56
Variance	76.7%	12.3%	5.2%	70.4%	24.7%	77.7%	9.2%	6.3%	6.2%
Cumulative variance	76.7%	89.0%	94.2%	70.4%	95.1%	77.7%	86.9%	93.2%	99.4%

and Cu was not statistically significant due to the limitation of sample numbers in this study, so this anthropogenic contribution of Fe deserves further investigation.

3.3.3 Principal Component Analysis (PCA) and Cluster Analysis (CA)

Table 4 shows the principal components (PC) of the valence states of target metals from XAFS. Eigenvalues, variance contributions, and cumulative variance are also presented. We also performed CA on target metal compounds for the three sites to better identify possible emission sources (Fig. 4). We performed PCA and CA for both particle sizes together because the number of samples was limited and because the irregular Cr concentration in PF collected in summer at SA had to be removed. The PCA and CA results for the three sites were different, even for KO and SA, which were relatively close geographically. This indicates that the emitting sources at each site were different and depended on their geographical location and regional characteristics.

For KO, the PCA model extracted three PCs and explained up to 94% of the total variance. PC1 and PC2 contained the most pollutant components, as their combined cumulative variance contribution reached 89.0%. The components originally belonging to PC1 were grouped into one cluster with those of PC2 in the CA analysis results. As previous discussion of emission sources of included factors, PC1 indicated the surface dust emission sources, including Cu(II) and Zn(II) generated from traffic brake wear, Mn(II), Fe(II), and Fe(III) from crustal soil. In combination with the CA results, Fe(II) and Fe(III) were also classified into the same cluster with

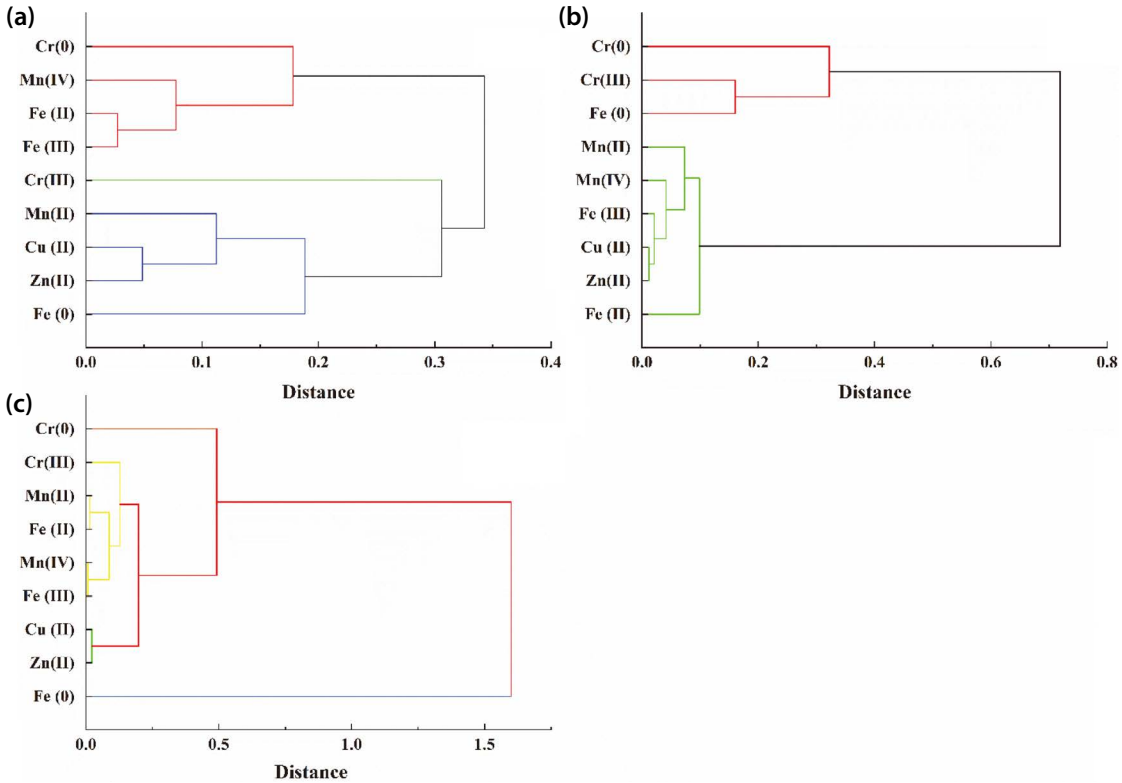

Fig. 4. Cluster analysis of target metal compounds from (a) KO, (b) SA, and (c) FU.

Cr(0) and Mn(IV) in PC2, this means possible anthropogenic activities emitting such as fly ash generated from steel and marine industries in the Keihin industrial area. The PCA and CA results show that Cr(III) was unique, it was always grouped separately and the variance contribution was 5.2% for PCA. There were strong correlations of Cr(III) with V, Ni, Cu, and Pb (Table 3a). Ni and V are often considered to be tracers of ship emissions because both are major impurities in residual oil used by ocean-going vessels, and shipping facilities are considered an important source of airborne fine Ni and V in port areas (Tian *et al.*, 2013; Peltier *et al.*, 2009), while Cu and Pb are the main elements in fly ash from municipal waste incinerators, and the crystalline and non-crystalline forms of Cr and Cu can be incorporated into the spinel structure in fly ash particles (Dahlan *et al.*, 2020; Takaoka *et al.*, 2016; Jung *et al.*, 2004; Wiles, 1996). Therefore, PC3 containing only Cr(III) can be considered to represent the combustion source such as fossil fuel burning and waste incineration.

At SA, the overall variance contribution of the two PCs was 95.1%. The PCA and CA results for the valence states were also consistent. This indicates that the sources of pollutants in this region were relatively stable, and the emission sources derived from the model results are sufficient to identify the largest sources of the target contaminants. The components of PC1 for SA and KO were similar. However, since Saitama Prefecture is an inland-type region with more developed agricultural production, the valence distribution of Mn and Fe, which mainly originate from the soil, maybe more related to the solidification process of toxic metals, which occurs in paddy soils during rice cultivation. Manganese oxides can alter the valence states of other heavy metals, such as arsenic (Oscarson *et al.*, 1983a, 1983b). For example, the reduction of Mn(IV) to Mn(II) oxidizes As(III) to As(V), and oxidation of As(III) by Mn oxides likely leads to decreased As mobility in soil (Lafferty *et al.*, 2010a, 2010b). Mn oxides would also promote Fe(II) oxidation to Fe(III), thereby creating freshly precipitated Fe(III) hydroxides that could serve as efficient sorbents for As (Xu *et al.*, 2017; Ehlert *et al.*, 2016). Some Mn-containing pesticides also contribute to the PM-bound Mn besides the soil re-suspension (Sysalova *et al.*, 2012). This might explain why the highest concentrations of Mn(II) and Fe(III) were found in SA samples in summer and autumn

when rice harvesting can cause more soil dust to enter the atmosphere. PC2 including the Cr(0), Cr(III), and Fe(0) might indicate the industrial emission source around the sampling site, and/or abrasion of metallic alloys on surfaces.

For FU, the PCA results were complex. For example, Fe(0) and Cu(II) had relatively high loadings in different PCs, and their PCA and CA results differed significantly. This was probably due to the diverse industrial structure of the Fukuoka region and its proximity to the East Asian continent, which makes it susceptible to long-distance transport of pollutants from the continent. Therefore, the sources of pollutants are more complex. The small number of samples (n = 7) obtained at FU may be another reason behind the large differences between the PCA and CA results. PCA is designed to capture the maximum amount of raw information and reduce the number of variables by extracting the main components of multivariate data, while CA groups variables that are close together into the same cluster in the dendrogram.

In terms of source identification of contaminants at FU, Cu(II) and Zn(II) were likely emitted from traffic brake wear. Cr(III), Mn(II), Mn(IV), Fe(II), and Fe(III) in aerosol particles were likely influenced by fly ash generated by steel production in the Kitakyushu industrial area, as previously discussed. Furthermore, the high correlation of Mn(II), Mn(IV), and Fe(III) with Ti indicate that they may have been from peri-urban agricultural production emissions. The CA results showed that Cr(0) and Fe(0) belonged to separate clusters, with low correlations between them and other pollutants but they were grouped in PC4 with Cu(II) and Zn(II) by PCA result. Kennedy and Gaddy (2003) presented that brake dust generated during the braking process wear of the brake discs/drums, which are commonly made of steel of alloys was enriched in Cr, Cu, Fe, and tin (Sn). This might indicate the unique sources for Cr(0) and Fe(0), such as the abrasion of metallic alloys on surfaces.

4. CONCLUSION

This study investigated the chemical compositions and valence states of elements in cyclone-collected particles from three sites in Japan. The average concentration of Fe was the highest among the nine metallic elements, and the ambient concentrations of Cu, Zn, and Pb far exceeded the background concentrations. XAFS results for the target metals showed that the major valence states were Cr(III), Mn(II), Fe(III), Cu(II), and Zn(II), followed by Cr(0), Mn(IV), Fe(II), Fe(0), and Cu(0). Cr(VI), Mn(0), and Zn(0) were detected in some samples, and Cu(I) was not detected in this study. Moreover, the source identification results from correlation analysis, PCA, and CA showed that the potential emission sources of metallic contaminants differed significantly across the three sites and suggested influence from industrial activities and geographical location. The main contribution source of Mn and Fe is crustal soil. At KO and FU, which are metropolises near the sea and adjacent to industrial areas, the probably anthropogenic sources of metal contaminants such as Cr(III), Mn(II), Mn(IV), Fe(II), and Fe(III) are likely fly ash from steel production and fuel combustion in industrial areas. At SA, which is located inland with greater agricultural production, the dominant source is likely soil dust from agricultural production but this hypothesis needs further research. The main source of Cu(II) and Zn(II) in all three areas can be traffic brake wear. In addition, the source analysis model showed that the pollutants in FU exhibited cross-regional transport characteristics. Our findings on the different valence states and compositions of the elements determined by cyclone collection coupled with XAFS and EDXRF may be important for determining the toxicity of PM at different locations.

ACKNOWLEDGEMENT

Part of this research was supported by the Environmental Research and Technology Development Fund of the Environmental Restoration and Conservation Agency (ERCA) (JPMEERF20165051 and JPMEERF20205007), JST CREST (JPMJCR19H3), JSPS KAKENHI Grant Numbers JP17H04480, JP18K19856, JP20H00636, JP20K20614, the Keio Leading-edge Laboratory Science and Technology Specified Research Projects, and Steel Foundation for Environmental Protection Technology. The experiments using synchrotron radiation were performed at the beamlines BL11 and BL15 of the SAGA Light Source with the proposal Nos. 1905032F, 1910086F, 1911105F, 2005039F, 2009097F, 2101001F, 2105038F (for BL11), and 2108109F (for BL15). We would like to thank Dr. H. Setoyama of SAGA-LS for technical assistance in operating XAFS measurement.

REFERENCES

Agrawal, H., Malloy, Q.G., Welch, W.A., Wayne Miller, J., Cocker, D.R. (2008a) In-use gaseous and particulate matter emissions from a modern ocean going container vessel. Atmospheric Environment, 42(21), 5504–5510. https://doi.org/10.1016/j.atmosenv.2008.02.053

Agrawal, H., Welch, W.A., Miller, J.W., Cocker, D.R. (2008b) Emission Measurements from a Crude Oil Tanker at Sea. Environmental Science & Technology, 42(19), 7098–7103. https://doi.org/10.1021/es703102y

Al-Momani, I.F., Daradkeh, A.S., Haj-Hussein, A.T., Yousef, Y.A., Jaradat, Q.M., Momani, K.A. (2005) Trace elements in daily collected aerosols in Al-Hashimya, central Jordan. Atmospheric Research, 73(1), 87–100. https://doi.org/10.1016/j.atmosres.2003.09.009

Alves, D.D., Riegel, R.P., Klauck, C.R., Ceratti, A.M., Hansen, J., Cansi, L.M., Pozza, S.A., de Quevedo, D.M., Osório, D.M.M. (2020) Source apportionment of metallic elements in urban atmospheric particulate matter and assessment of its water-soluble fraction toxicity. Environmental Science and Pollution Research International, 27(11), 12202–12214. https://doi.org/10.1007/s11356-020-07791-8

Amato, F., Cassee, F.R., Denier van der Gon, H.A., Gehrig, R., Gustafsson, M., Hafner, W., Harrison, R.M., Jozwicka, M., Kelly, F.J., Moreno, T., Prevot, A.S.H., Schaap, M., Sunyer, J., Querol, X. (2014) Urban air quality: The challenge of traffic non-exhaust emissions. Journal of Hazardous Materials, 275, 31–36. https://doi.org/10.1016/j.jhazmat.2014.04.053

Bardelli, F., Cattaruzza, E., Gonella, F., Rampazzo, G., Valotto, G. (2011) Characterization of road dust collected in Traforo del San Bernardo highway tunnel: Fe and Mn speciation. Atmospheric Environment, 45(35), 6459–6468. https://doi.org/10.1016/j.atmosenv.2011.07.035

Charlson, F., Ferrari, A., Fullman, N., Reitsma, M., Vos, T., Zhou, M., Abajobir, A., Abd-Allah, F., Aldhahri, S., Alemu, Z., Alla, F., Allebeck, P., Martin, E., Atique, S., Quintanilla, B., Barquera, S., Basu, S., Beghi, E., Bell, M., … Brugha, T. (2016) Global, regional, and national comparative risk assessment of 79 behavioural, environmental and occupational, and metabolic risks or clusters of risks, 1990–2015: a systematic analysis for the Global Burden of Disease Study 2015. The Lancet, 388(10053), 1659–1724. https://doi.org/10.1016/S0140-6736(16)31679-8

Chen, H., Lu, X., Li, L.Y., Gao, T., Chang, Y. (2014) Metal contamination in campus dust of Xi'an, China: A study based on multivariate statistics and spatial distribution. The Science of the Total Environment, 484, 27–35. https://doi.org/10.1016/j.scitotenv.2014.03.026

Chen, X., Guo, M., Feng, J., Liang, S., Han, D., Cheng, J. (2019) Characterization and risk assessment of heavy metals in road dust from a developing city with good air quality and from Shanghai, China. Environmental Science and Pollution Research International, 26(11), 11387–11398. https://doi.org/10.1007/s11356-019-04550-2

Chirizzi, D., Cesari, D., Guascito, M., Dinoi, A., Giotta, L., Donateo, A., Contini, D. (2017) Influence of Saharan dust outbreaks and carbon content on oxidative potential of water-soluble fractions of $PM_{2.5}$ and PM_{10}. Atmospheric Environment, 163, 1–8. https://doi.org/10.1016/j.atmosenv.2017.05.021

Chowdhury, P.H., Honda, A., Ito, S., Okano, H., Onishi, T., Higashihara, M., Okuda, T., Tanaka, T., Hirai, S., Takano, H. (2019) Effects of ambient $PM_{2.5}$ collected from Asian cities using cyclone technique on human airway epithelial cells. Aerosol and Air Quality Research, 19(8), 1808–1819. https://doi.org/10.4209/aaqr.2019.01.0016

Cohen, A., Brauer, M., Burnett, R., Anderson, H., Frostad, J., Estep, K., Balakrishnan, K., Brunekreef, B., Dandona, L., Dandona, R., Feigin, V., Freedman, G., Hubbell, B., Jobling, A., Kan, H., Knibbs, L., Liu, Y., Martin, R., Morawska, L., Arden Pope III, C., Shin, H., Straif, K., Shaddick, G., Thomas, M., van Dingenen, R., van Donkelaar, A., Vos, T., Murray, C.J.L., Forouzanfar, M. (2017) Estimates and 25-year trends of the global burden of disease attributable to ambient air pollution: an analysis of data from the Global Burden of Diseases Study 2015. The Lancet, 389(10082), 1907–1918. https://doi.org/10.1016/S0140-6736(17)30505-6

Cohen, M.D., Sisco, M., Prophete, C., Chen, L., Zelikoff, J.T., Ghio, A.J., Stonehuerner, J.D., Smee, J.J., Holder, A.A., Crans, D.C. (2007) Pulmonary Immunotoxic Potentials of Metals Are Governed by Select Physicochemical Properties: Vanadium Agents. Journal of Immunotoxicology, 4(1), 49–60. https://doi.org/10.1080/15476910601119350

Dahlan, A.V., Kitamura, H., Sakanakura, H., Shimaoka, T., Yamamoto, T., Takahashi, F. (2020) Possible metal speciation in the fly ash produced from a fluidized bed incinerator of municipal solid waste. In Proceedings of the Annual Conference of the 31st Japan Society of Material Cycles and Waste Management (p. 505–506). Japan Society of Material Cycles and Waste Management.

Ehlert, K., Mikutta, C., Kretzschmar, R. (2016) Effects of Manganese Oxide on Arsenic Reduction and Leaching from Contaminated Floodplain Soil. Environmental Science & Technology, 50(17), 9251–9261. https://doi.org/10.1021/acs.est.6b01767

Furutani, H., Jung, J., Miura, K., Takami, A., Kato, S., Kajii, Y., Uematsu, M. (2011) Single-particle chemical characterization and source apportionment of iron-containing atmospheric aerosols in Asian outflow. Journal of Geophysical Research: Atmospheres, 116(D18). https://doi.org/10.1029/2011JD015867

Gao, D., Pollitt, K.J.G., Mulholland, J.A., Russell, A.G., Weber, R.J. (2020) Characterization and comparison of $PM_{2.5}$ oxidative potential assessed by two acellular assays. Atmospheric Chemistry and Physics, 20(9), 5197–5210. https://doi.org/10.5194/acp-20-5197-2020

Grigoratos, T., Martini, G. (2015) Brake wear particle emissions: a review. Environmental Science and Pollution Research International, 22(4), 2491–2504. https://doi.org/10.1007/s11356-014-3696-8

Harrison, R.M., Deacon, A.R., Jones, M.R., Appleby, R.S. (1997) Sources and processes affecting concentrations of PM_{10} and $PM_{2.5}$ particulate matter in Birmingham (U.K.). Atmospheric Environment, 31(24), 4103–4117. https://doi.org/10.1016/S1352-2310(97)00296-3

Hassan, S.K.M. (2012) Metal concentrations and distribution in the household, stairs and entryway dust of some Egyptian homes. Atmospheric Environment, 54, 207–215. https://doi.org/10.1016/j.atmosenv.2012.02.013

Hassanvand, M.S., Naddafi, K., Faridi, S., Nabizadeh, R., Sowlat, M.H., Momeniha, F., Gholampour, A., Arhami, M., Kashani, H., Zare, A., Niazi, S., Rastkari, N., Nazmara, S., Ghani, M., Yunesian, M. (2015) Characterization of PAHs and metals in indoor/outdoor $PM_{10}/PM_{2.5}/PM_1$ in a retirement home and a school dormitory. The Science of the Total Environment, 527–528, 100–110. https://doi.org/10.1016/j.scitotenv.2015.05.001

Havlík, T., Souza, B.V.e, Bernardes, A.M., Schneider, I.A.H., Miškufová, A. (2006) Hydrometallurgical processing of carbon steel EAF dust. Journal of Hazardous Materials, 135 (1), 311–318. https://doi.org/10.1016/j.jhazmat.2005.11.067

Hering, S.V., Appel, B.R., Cheng, W., Salaymeh, F., Cadle, S.H., Mulawa, P.A., Cahill, T.A., Eldred, R.A., Surovik, M., Fitz, D., Howes, J.E., Knapp, K.T., Stockburger, L., Turpin, B.J., Huntzicker, J.J., Zhang, X.-Q., McMurry, P.H. (1990) Comparison of Sampling Methods for Carbonaceous Aerosols in Ambient Air. Aerosol Science and Technology, 12(1), 200–213. https://doi.org/10.1080/02786829008959340

Honda, A., Okuda, T., Nagao, M., Miyasaka, N., Tanaka, M., Takano, H. (2021) $PM_{2.5}$ collected using cyclonic separation causes stronger biological responses than that collected using a conventional filtration method. Environmental Research, 198, 110490. https://doi.org/10.1016/j.envres.2020.110490

Huggins, F.E., Huffman, G.P. (2002) X-ray Absorption Fine Structure (XAFS) Spectroscopic Characterization of Emissions from Combustion of Fossil Fuels. International Journal of the Society of Materials Engineering for Resources, 10(1), 1–13. https://doi.org/10.5188/ijsmer.10.1

Iijima, A., Sato, K., Yano, K., Tago, H., Kato, M., Kimura, H., Furuta, N. (2007) Particle size and composition distribution analysis of automotive brake abrasion dusts for the evaluation of antimony sources of airborne particulate matter. Atmospheric Environment, 41(23), 4908–4919. https://doi.org/10.1016/j.atmosenv.2007.02.005

Janssen, N.A.H., Yang, A., Strak, M., Steenhof, M., Hellack, B., Gerlofs-Nijland, M.E., Kuhlbusch, T., Kelly, F., Harrison, R., Brunekreef, B., Hoek, G., Cassee, F. (2014) Oxidative potential of particulate matter collected at sites with different source characteristics. The Science of the Total Environment, 472, 572–581. https://doi.org/10.1016/j.scitotenv.2013.11.099

Japan Mateorological Agency (JAM) (2021) https://www.data.jma.go.jp/obd/stats/etrn/view/mb5daily_s1.php?prec_no=46&block_no=47670&year=2017&month=&day=&view=a1

Jeong, H., Ra, K., Kim, K.-T., Kim, E.-S., Lee, S.-Y., Choi, M.-S. (2018) Tracing the Pollution Source Using Pb Isotopes in Sediments of the Coastal Region Surrounding the National Industrial Complex, Korea. Journal of Coastal Research, 85(85), 1456–1460. https://doi.org/10.2112/SI85-292.1

Jung, C.H., Matsuto, T., Tanaka, N., Okada, T. (2004) Metal distribution in incineration residues of municipal solid waste (MSW) in Japan. Waste Management, 24(4), 381–391. https://doi.org/10.1016/S0956-053X(03)00137-5

Kaneyasu, N., Yamamoto, S., Sato, K., Takami, A., Hayashi, M., Hara, K., Kawamoto, K., Okuda, T., Hatakeyama, S. (2014) Impact of long-range transport of aerosols on the $PM_{2.5}$ composition at a major metropolitan area in the northern Kyushu area of Japan. Atmospheric Environment, 97, 416–425. https://doi.org/10.1016/j.atmosenv.2014.01.029

Kennedy, P., Gadd, J. (2003) Preliminary examination of trace elements in tyres, brake pads, and road bitumen in New Zealand. Prepared for Ministry of Transport, New Zealand, Infrastructure Auckland.

Kristensen, K., Bilde, M., Aalto, P.P., Petäjä, T., Glasius, M. (2016) Denuder/filter sampling of organic acids and organosulfates at urban and boreal forest sites: Gas/particle distribution and possible sampling artifacts. Atmospheric Environment, 130(C), 36–53. https://doi.org/10.1016/j.atmosenv.2015.10.046

Lafferty, B.J., Ginder-Vogel, M., Sparks, D.L. (2010) Arsenite Oxidation by a Poorly Crystalline Manganese-Oxide 1. Stirred-Flow Experiments. Environmental Science & Technology, 44(22), 8460–8466. https://doi.org/10.1021/es102013p

Lafferty, B.J., Ginder-Vogel, M., Zhu, M., Livi, K.J.T., Sparks, D.L. (2010) Arsenite Oxidation by a Poorly Crystalline Manganese-Oxide. 2. Results from X-ray Absorption Spectroscopy and X-ray Diffraction. Environmental Science & Technology, 44(22), 8467–8472. https://doi.org/10.1021/es102016c

Li, R., Ning, Z., Majumdar, R., Cui, J., Takabe, W., Jen, N., Sioutas, C., Hsiai, T. (2010) Ultrafine particles from diesel vehicle emissions at different driving cycles induce differential vascular pro-inflammatory responses: implication of chemical components and NF-kappaB signaling. Particle and Fibre Toxicology, 7, 6. https://doi.org/10.1186/1743-8977-7-6

López, M.L., Ceppi, S., Palancar, G.G., Olcese, L.E., Tirao, G., Toselli, B.M. (2011) Elemental concentration and source identification of PM_{10} and $PM_{2.5}$ by SR-XRF in Córdoba City. Argentina. Atmospheric Environment, 45(31), 5450–5457. https://doi.org/10.1016/j.atmosenv.2011.07.003

Loska, K., Cebula, J., Pelczar, J., Wiechua, D., Kwapuliski, J. (1997) Use of enrichment, and contamination factors together with geoaccumulation indexes to evaluate the content of Cd, Cu, and Ni in the Rybnik Water Reservoir in Poland. Water, Air and Soil Pollution, 93(1–4), 347–365. https://doi.org/10.1023/A:1022121615949

Lu, X., Wang, L., Lei, K., Huang, J., Zhai, Y. (2009) Contamination assessment of copper, lead, zinc, manganese and nickel in street dust of Baoji, NW China. Journal of Hazardous Materials, 161(2), 1058–1062. https://doi.org/10.1016/j.jhazmat.2008.04.052

Manno, E., Varrica, D., Dongarrà, G. (2006) Metal distribution in road dust samples collected in an urban area close to a petrochemical plant at Gela, Sicily. Atmospheric Environment, 40(30), 5929–5941. https://doi.org/10.1016/j.atmosenv.2006.05.020

Marcoccia, M., Ronci, L., De Matthaeis, E., Setini, A., Perrino, C., Canepari, S. (2017) In-vivo assesment of the genotoxic and oxidative stress effects of particulate matter on Echino-

gammarus veneris. Chemosphere, 173, 124–134. https://doi.org/10.1016/j.chemosphere.2017.01.019

Ny, M.T., Lee, B.-K. (2010) Size Distribution and Source Identification of Airborne Particulate Matter and Metallic Elements in a Typical Industrial City. Asian Journal of Atmospheric Environment, 4(1), 9–19. https://doi.org/10.5572/ajae.2010.4.1.009

Ogino, K., Nagaoka, K., Ito, T., Takemoto, K., Okuda, T., Nakayama, S., Ogino, N., Seki, Y., Hamada, H., Takashiba, S., Fujikura, Y. (2018) Involvement of $PM_{2.5}$-bound protein and metals in $PM_{2.5}$-induced allergic airway inflammation in mice. Inhalation Toxicology, 30(13–14), 498–508. https://doi.org/10.1080/08958378.2018.1561769

Ogino, K., Nagaoka, K., Okuda, T., Oka, A., Kubo, M., Eguchi, E., Fujikura, Y. (2017) $PM_{2.5}$-induced airway inflammation and hyperresponsiveness in NC/Nga mice. Environmental Toxicology, 32(3), 1047–1054. https://doi.org/10.1002/tox.22303

Ohta, A., Tsuno, H., Kagi, N., Kanai, Y., Nomura, M., Zhang, R.J., Terashima, G., Imai, N. (2006) Chemical compositions and XANES speciations of Fe, Mn and Zn from aerosols collected in China and Japan during dust events. Geochemical Journal, 40, 363-376. https://doi.org/10.2343/geochemj.40.363

Okuda, T. (2013) Measurement of the specific surface area and particle size distribution of atmospheric aerosol reference materials. Atmospheric Environment, 75, 1–5. https://doi.org/10.1016/j.atmosenv.2013.04.033

Okuda, T., Isobe, R. (2017) Improvement of a High-volume Aerosol Particle Sampler for Collecting Submicron Particles through the Combined Use of a Cyclone with a Smoothened Inner Wall and a Circular Cone Attachment. Asian Journal of Atmospheric Environment, 11(2), 131–137. https://doi.org/10.5572/ajae.2017.11.2.131

Okuda, T., Fujimori, E., Hatoya, K., Takada, H., Kumata, H., Nakajima, F., Hatakeyama, S., Uchida, M., Tanaka, S., He, K., Ma, Y., Haraguchi, H. (2013) Rapid and Simple Determination of Multi-Elements in Aerosol Samples Collected on Quartz Fiber Filters by Using EDXRF Coupled with Fundamental Parameter Quantification Technique. Aerosol and Air Quality Research, 13(6), 1864–1876. https://doi.org/10.4209/aaqr.2012.11.0308

Okuda, T., Isobe, R., Nagai, Y., Okahisa, S., Funato, K., Inoue, K. (2015) Development of a high-volume $PM_{2.5}$ particle sampler using impactor and cyclone techniques. Aerosol and Air Quality Research, 15(3), 759–767. https://doi.org/10.4209/aaqr.2014.09.0194

Okuda, T., Katsuno, M., Naoi, D., Nakao, S., Tanaka, S., He, K., Ma, Y., Lei, Y., Jia, Y. (2008) Trends in hazardous trace metal concentrations in aerosols collected in Beijing, China from 2001 to 2006. Chemosphere, 72(6), 917–924, https://doi.org/10.1016/j.chemosphere.2008.03.033

Okuda, T., Shishido, D., Terui, Y., Fujioka, K., Isobe, R., Iwaki, Y., Funato, K., Inoue, K. (2018) Development of a high-volume simultaneous sampler for fine and coarse particles using virtual impactor and cyclone techniques. Asian Journal of Atmospheric Environment, 12(1), 78–86. https://doi.org/10.5572/ajae.2018.12.1.078.

Omran, M., Fabritius, T. (2017) Effect of steelmaking dust characteristics on suitable recycling process determining: Ferrochrome converter (CRC) and electric arc furnace (EAF) dusts. Powder Technology, 308, 47–60. https://doi.org/10.1016/j.powtec.2016.11.049

Oscarson, D.W., Huang, P.M., Liaw, W.K., Hammer, U.T. (1983a) Kinetics of oxidation of arsenite by various manganese dioxides. Soil Science Society of America Journal, 47(4), 644–648. https://doi.org/10.2136/sssaj1983.03615995004700040007x

Oscarson, D.W., Huang, P.M., Hammer, U.T., Liaw, W.K. (1983b) Oxidation and sorption of arsenite by manganese dioxide as influenced by surface coatings of iron and aluminum oxides and calcium carbonate. Water, Air, and Soil Pollution, 20, 233–244. https://doi.org/10.1007/BF00279633

Oustadakis, P., Tsakiridis, P.E., Katsiapi, A., Agatzini-leonardou, S. (2010) Hydrometallurgical process for zinc recovery from electric arc furnace dust (EAFD) Part I: Characterization and leaching by diluted sulphuric acid. Journal of Hazardous Materials, 179(1–3), 1–7. https://doi.org/10.1016/j.jhazmat.2010.01.059

Pandey, M., Pandey, A.K., Mishra, A., Tripathi, B.D. (2017) Speciation of carcinogenic and non-carcinogenic metals in respirable suspended particulate matter (PM_{10}) in Varanasi, India. Urban Climate, 19, 141–154. https://doi.org/10.1016/j.uclim.2017.01.004

Parshintsev, J., Ruiz-Jimenez, J., Petäjä, T., Hartonen, K., Kulmala, M., Riekkola, M.-L. (2011) Comparison of quartz and Teflon filters for simultaneous collection of size-separated ultrafine aerosol particles and gas-phase zero samples. Analytical and Bioanalytical Chemistry, 400(10), 3527–3535. https://doi.org/10.1007/s00216-011-5041-0

Peltier, R.E., Hsu, S.-I., Lall, R., Lippmann, M. (2009) Residual oil combustion: a major source of airborne nickel in New York City. Journal of Exposure Science & Environmental Epidemiology, 19(6), 603–612. https://doi.org/10.1038/jes.2008.60

Piscitello, A., Bianco, C., Casasso, A., Sethi, R. (2021) Non-exhaust traffic emissions: Sources, characterization, and mitigation measures. The Science of the Total Environment, 766, 144440. https://doi.org/10.1016/j.scitotenv.2020.144440

Roper, C., Delgado, L., Barrett, D., Massey Simonich, S., Tanguay, R. (2019) $PM_{2.5}$ Filter Extraction Methods: Implications for Chemical and Toxicological Analyses. Environmental Science & Technology, 53(1), 434–442. https://doi.org/10.1021/acs.est.8b04308

Safai, P., Raju, M., Rao, P., Pandithurai, G. (2014) Characterization of carbonaceous aerosols over the urban tropical location and a new approach to evaluate their climatic importance. Atmospheric Environment, 92, 493–500. https://doi.org/10.1016/j.atmosenv.2014.04.055

Sagawa, T., Tsujikawa, T., Honda, A., Miyasaka, N., Tanaka, M., Kida, T., Hasegawa, K., Okuda, T., Kawahito, Y., Takano, H. (2021) Exposure to particulate matter upregulates ACE2 and TMPRSS2 expression in the murine lung. Environmental Research, 195, 110722. https://doi.org/10.1016/j.envres.2021.110722

Saito, K., Okuda, T., Hasegawa, S., Nishita-Hara, C., Hara, K.,

Hayashi, M. (2020) Chemical Speciation of Chromium in Atmospheric Particulate Matter Collected with Cyclone by XAFS Method. Journal of Japan Society for Atmospheric Environment, 55(2), 27–33, (in Japanese with English Abstract). https://doi.org/10.11298/taiki.55.27

Sakata, M., Xu, H., Mashio, A.S. (2018) Analysis of historical trend of pollution sources of lead in Tokyo Bay based on lead isotope ratios in sediment core. Journal of Oceanography, 74(2), 187–196. https://doi.org/10.1007/s10872-017-0448-7

See, S., Wang, Y.H., Balasubramanian, R. (2007) Contrasting reactive oxygen species and transition metal concentrations in combustion aerosols. Environmental Research, 103(3), 317–324. https://doi.org/10.1016/j.envres.2006.08.012

Shahpoury, P., Zhang, Z., Arangio, A., Celo, V., Dabek-Zlotorzynska, E., Harner, T., Nenes, A. (2021) The influence of chemical composition, aerosol acidity, and metal dissolution on the oxidative potential of fine particulate matter and redox potential of the lung lining fluid. Environment International, 148, 106343. https://doi.org/10.1016/j.envint.2020.106343

Sheehan, P.J., Meyer, D.M., Sauer, M.M., Paustenbach, D.J. (1991) Assessment of the human health risks posed by exposure to chromium-contaminated soils. Journal of Toxicology and Environmental Health, 32(2), 161–201. https://doi.org/10.1080/15287399109531476

Shimada, K., Yang, X., Araki, Y., Yoshino, A., Takami, A., Chen, X., Meng, F., Hatakeyama, S. (2018) Concentrations of metallic elements in long-range-transported aerosols measured simultaneously at three coastal sites in China and Japan. Journal of Atmospheric Chemistry, 75(2), 123–139. https://doi.org/10.1007/s10874-017-9366-8

Sofilić, T., Rastovčan-Mioč, A., Cerjan-Stefanović, Š., Novosel-Radović, V., Jenko, M. (2004) Characterization of steel mill electric-arc furnace dust. Journal of Hazardous Materials, 109(1), 59–70. https://doi.org/10.1016/j.jhazmat.2004.02.032

Stoiber, T.L., Shafer, M.M., Armstrong, D.E. (2013) Induction of reactive oxygen species in chlamydomonas reinhardtii in response to contrasting trace metal exposures. Environmental Toxicology, 28(9), 516–523. https://doi.org/10.1002/tox.20743

Sugiyama, T., Ueda, K., Seposo, X., Nakashima, A., Kinoshita, M., Matsumoto, H., Ikemori, F., Honda, A., Takano, H., Michikawa, T., Nitta, H. (2020) Health effects of $PM_{2.5}$ sources on children's allergic and respiratory symptoms in Fukuoka, Japan. The Science of the Total Environment, 709, 136023. https://doi.org/10.1016/j.scitotenv.2019.136023

Sun, H., Brocato, J., Costa, M. (2015) Oral Chromium Exposure and Toxicity. Current Environmental Health Reports, 2(3), 295–303. https://doi.org/10.1007/s40572-015-0054-z

Sun, Q., Hong, X., Wold, L. (2010) Cardiovascular Effects of Ambient Particulate Air Pollution Exposure. Circulation, 121(25), 2755–2765. https://doi.org/10.1161/CIRCULATIONAHA.109.893461

Sun, Y., Wang, Z., Fu, P., Jiang, Q., Yang, T., Li, J., Ge, X. (2013) The impact of relative humidity on aerosol composition and evolution processes during wintertime in Beijing, China. Atmospheric Environment, 77, 927–934. https://doi.org/10.1016/j.atmosenv.2013.06.019

Sysalova, J., Sykorova, I., Havelcova, M., Szakova, J., Trejtnarova, H., Kotlik, B. (2012) Toxicologically important trace elements and organic compounds investigated in size-fractionated urban particulate matter collected near the Prague highway. The Science of the Total Environment, 437, 127–136. https://doi.org/10.1016/j.scitotenv.2012.07.030

Szigeti, T., Óvári, M., Dunster, C., Kelly, F.J., Lucarelli, F., Záray, G. (2015) Changes in chemical composition and oxidative potential of urban $PM_{2.5}$ between 2010 and 2013 in Hungary. The Science of the Total Environment, 518–519, 534–544. https://doi.org/10.1016/j.scitotenv.2015.03.025

Taghvaee, S., Sowlat, M., Diapouli, E., Manousakas, M., Vasilatou, V., Eleftheriadis, K., Sioutas, C. (2019) Source apportionment of the oxidative potential of fine ambient particulate matter ($PM_{2.5}$) in Athens, Greece. The Science of the Total Environment, 653, 1407–1416. https://doi.org/10.1016/j.scitotenv.2018.11.016

Takahashi, Y., Higashi, M., Furukawa, T., Mitsunobu, S. (2011) Change of iron species and iron solubility in Asian dust during the long-range transport from western China to Japan. Atmospheric Chemistry and Physics, 11, 11237–11252. https://doi.org/10.5194/acp-11-11237-2011

Takaoka, M., Shiota, K., Imai, G., Oshita, K. (2016) Emission of particulate matter 2.5 ($PM_{2.5}$) and elements from municipal solid waste incinerators. Journal of Material Cycles and Waste Management, 18(1), 72–80. https://doi.org/10.1007/s10163-014-0314-2

Tanner, P.A., Ma, H.-L., Yu, P.K.N. (2008) Fingerprinting Metals in Urban Street Dust of Beijing, Shanghai, and Hong Kong. Environmental Science & Technology, 42(19), 7111–7117. https://doi.org/10.1021/es8007613

Taylor, M., Kruger, N. (2020) Tyre Weights an Overlooked Diffuse Source of Lead and Antimony to Road Runoff. Sustainability, 12(17), 6790. https://doi.org/10.3390/su12176790

Taylor, S. (1964) Abundance of chemical elements in the continental crust: a new table. Geochimica et Cosmochimica Acta, 28(8), 1273–1285. https://doi.org/10.1016/0016-7037(64)90129-2

Tian, L., Ho, K., Louie, P.K., Qiu, H., Pun, V.C., Kan, H., Yu, I.T., Wong, T.W. (2013) Shipping emissions associated with increased cardiovascular hospitalizations. Atmospheric Environment, 74, 320–325. https://doi.org/10.1016/j.atmosenv.2013.04.014

Vallius, M., Lanki, T., Tiittanen, P., Koistinen, K., Ruuskanen, J., Pekkanen, J. (2003) Source apportionment of urban ambient $PM_{2.5}$ in two successive measurement campaigns in Helsinki, Finland. Atmospheric Environment, 37(5), 615–623. https://doi.org/10.1016/S1352-2310(02)00925-1

Van Winkle, L., Bein, K., Anderson, D., Pinkerton, K., Tablin, F., Wilson, D., Wexler, A. (2015) Biological dose response to $PM_{2.5}$: effect of particle extraction method on platelet and lung responses. Toxicological Sciences, 143(2), 349–359. https://doi.org/10.1093/toxsci/kfu230

Wang, F., Guo, Z., Lin, T., Hu, L., Chen, Y., Zhu, Y. (2015) Characterization of carbonaceous aerosols over the East China Sea: The impact of the East Asian continental outflow.

Atmospheric Environment, 110, 163–173. https://doi.org/10.1016/j.atmosenv.2015.03.059

Wang, Y., Plewa, M.J., Mukherjee, U.K., Verma, V. (2018) Assessing the cytotoxicity of ambient particulate matter (PM) using Chinese hamster ovary (CHO) cells and its relationship with the PM chemical composition and oxidative potential. Atmospheric Environment, 179, 132–141. https://doi.org/10.1016/j.atmosenv.2018.02.025

Wei, M., Li, M., Xu, C., Xu, P., Liu, H. (2020) Pollution characteristics of bioaerosols in $PM_{2.5}$ during the winter heating season in a coastal city of northern China. Environmental Science and Pollution Research International, 27(22), 27750–27761. https://doi.org/10.1007/s11356-020-09070-y

Wiles, C.C. (1996) Municipal solid waste combustion ash: State-of-the-knowledge. Journal of Hazardous Materials, 47(1), 325–344. https://doi.org/10.1016/0304-3894(95)00120-4

Xia, D.K., Picklesi, C.A. (2000) Microwave caustic leaching of electric arc furnace dust. Minerals Engineering, 13(1), 79–94. https://doi.org/10.1016/S0892-6875(99)00151-X

Xu, H., Cao, J., Ho, K., Ding, H., Han, Y., Wang, G., Chow, J., Watson, J., Khol, S., Qiang, J., Li, W.T. (2012) Lead concentrations in fine particulate matter after the phasing out of leaded gasoline in Xi'an, China. Atmospheric Environment, 46, 217–224. https://doi.org/10.1016/j.atmosenv.2011.09.078

Xu, X., Chen, C., Wang, P., Kretzschmar, R., Zhao, F.-J. (2017) Control of arsenic mobilization in paddy soils by manganese and iron oxides. Environmental Pollution, 231(Pt 1), 37–47. https://doi.org/10.1016/j.envpol.2017.07.084

Yuen, J.Q., Olin, P.H., Lim, H.S., Benner, S.G., Sutherland, R.A., Ziegler, A.D. (2012) Accumulation of potentially toxic elements in road deposited sediments in residential and light industrial neighborhoods of Singapore. Journal of Environmental Management, 101, 151–163. https://doi.org/10.1016/j.jenvman.2011.11.017

Zanobetti, A., Coull, B., Gryparis, A., Kloog, I., Sparrow, D., Vokonas, P., Wright, R., Gold, D., Schwartz, J. (2014) Associations between arrhythmia episodes and temporally and spatially resolved black carbon and particulate matter in elderly patients. Occupational and Environmental Medicine, 71(3), 201–207. https://doi.org/10.1136/oemed-2013-101526

Zhang, G. (2003) Atmospheric particulate matter studied by Mössbauer spectroscopy and XAFS. Hyperfine Interactions, 151(1), 299–306. https://doi.org/10.1023/B:HYPE.0000020421.68173.55